MANUFACTURE AND COMPRESSION TESTING OF A MACHINED COMPOSITE MECHANICAL SYSTEM

Thomas J. Rohrbach, Eltahry Elghandour

California Polytechnic State University, San Luis Obispo
Mechanical Engineering Dept.
San Luis Obispo, California

ABSTRACT

Exploration of this technology will be investigated through a combination of simulation, manufacturing, machining and testing. A steel connecting rod is used as a control case to which triaxially woven and discontinuous fiber composite materials are compared. Based on material testing with respect to elastic modulus and machinability the woven composite was selected as the primary material of interest for connecting rod geometry compression testing. The results of testing showed a failure load lower than of what is usually designed for, but a promising evaluation when compared to the steel component's strength to weight ratio.

1. INTRODUCTION

Composite materials hold great potential for the replacement of traditional materials in designs and machinery utilized on a daily basis. One such example is within an engine block assembly where massive components inherently reduce the effectiveness of the system they constitute. By replacing metal elements such as connecting rods, cylinder caps, or a crankshaft with composite alternatives, a significant increase in performance may be achieved with respect to mechanical strength, thermal stability, and durability while reducing mass [1]. By utilizing these beneficial aspects of composites the life of the components may be extended and the efficiency of the systems they comprise can be increased.

1.1 Connecting Rod

A connecting rod is a mechanism which connects and couples motion between components in a mechanism. A typical example is found in a combustion engine where the connecting rod translates the linear motion of a piston firing into the rotation of a crankshaft, as depicted in Figure 1. As a result of piston location in an engine the rod experiences extreme environments with respect to dynamic and thermal loading. However, due to the complex interactions of all of the resultant forces the focus of this study is scoped to only evaluate axial compressive load on the connecting rod to allow focus on

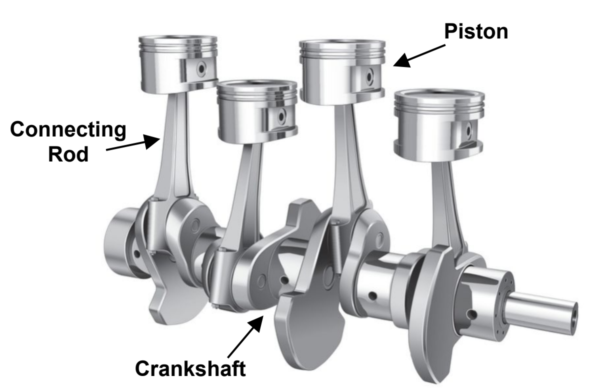

Figure 1 - Example of connecting rod in assembly [2]

Copyright 2019. Used by the Society of the Advancement of Material and Process Engineering with permission.

substitution of composite materials for the same geometry.

1.2 Composite Materials

A composite material is a material made up of two or more materials with different properties which remain distinct in the finished structure. Composite materials have many general applications such as aircraft/spacecraft systems, automotive parts, bridges, or electrical component housing. They are ideal for a number of applications due to their low mass and high strength/stiffness characteristics. Fibers used within composite systems come in a variety of styles and weaves including discontinuous/random orientation, unidirectional, and woven. The composites being examined within this study are a chopped fiber pre-impregnated system and a triaxially woven pre-impregnated system. Examples of the fiber orientations being studied are depicted in Figures 2 and 3 below, with the convention of the woven material orientation asserted as referenced throughout this paper. Typical unidirectional or woven fibers exhibit anisotropic characteristics meaning that the stress state in the material is dependent on the direction in which a load is applied. The advantage of exploring the two unique materials mentioned previously is their quasi-isotropic material behavior, meaning that the material exhibits nearly the name elastic properties regardless of the direction of in-plane loading. This is accomplished by the equal angular separation in the triaxial weave, and the random, discontinuous nature of the chopped fibers. This serves to benefit the concept of compression molding the material for machining geometry and maintaining favorable material behavior along the loading axis.

Figure 2 – Chopped carbon fiber [3]

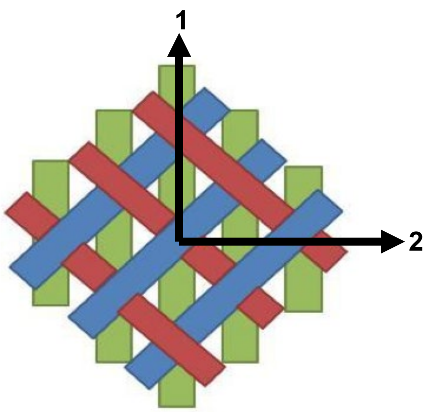

Figure 3 – Triaxial weave [4]

1.3 Scope of Work

The scope of the work conducted within this study covers a broad range of topics. Material selection was conducted based on criteria crucial to the intended final geometry and strength performance. Manufacturing efforts included compression molding experimentation, aluminum mold fabrication, and machining of connecting rod geometry from composite bricks. Experimental testing focused on characterization of material properties to guide composite selection for the machined connecting rods used in compression testing. Finite element analysis was conducted on the full geometry using the properties of steel for experimental verification and modeled geometry validation. Success of the composite substitution for the steel component was assessed through compressive failure testing and the resultant strength to weight ratio.

2. BASELINE MODELING AND VERIFICATION

A baseline for this study was established using a steel connecting rod taken from a Ford Vulcan V6 engine assembly. The component as seen in figure 4 was used to generate a CAD model pictured in Figure 5. This model was applied within FEA for experimental validation and utilized to generate tool pathing necessary for machining composite rods of the same geometry.

2.1 Compression Testing

Compression testing was conducted on an instrumented steel connecting rod using Micro-Measurement 120 Ohm strain gauges placed in particular areas of interest. By conducting compression testing a baseline of realistic experimental behavior could be used to verify the modeled geometry and loading conditions used in FEA.

The steel component was tested using an Instron hydraulic system. The system was instrumented with a load cell and a DAQ to display force readings. Strain gauge measurements were taken using a quarter bridge configuration through a strain gauge box, pictured in Figure 6. The rod shown in Figure 4 was mounted to the custom fixtures shown in Figure 7 to ensure proper loading on the specimen. Data recorded at 100 lbf intervals up to -1100 lbf total is exhibited in Figure 8.

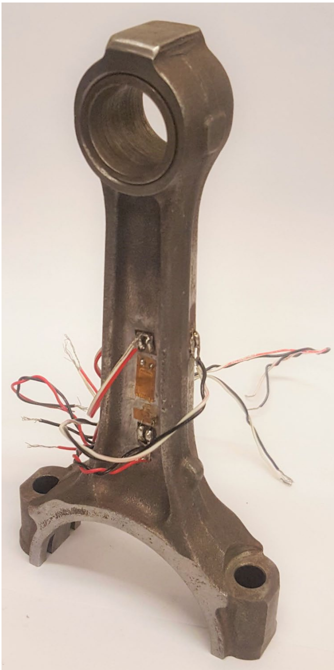

Figure 4 – Steel connecting rod

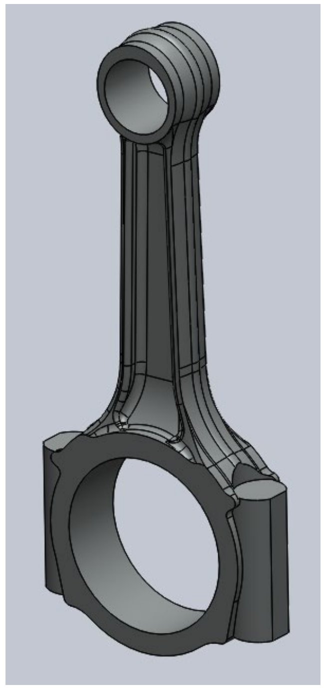

Figure 5 - Connecting rod CAD

Figure 6 – Strain gauge box

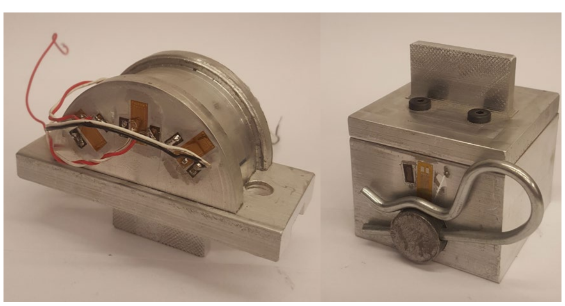

Figure 7 – Compression testing fixtures

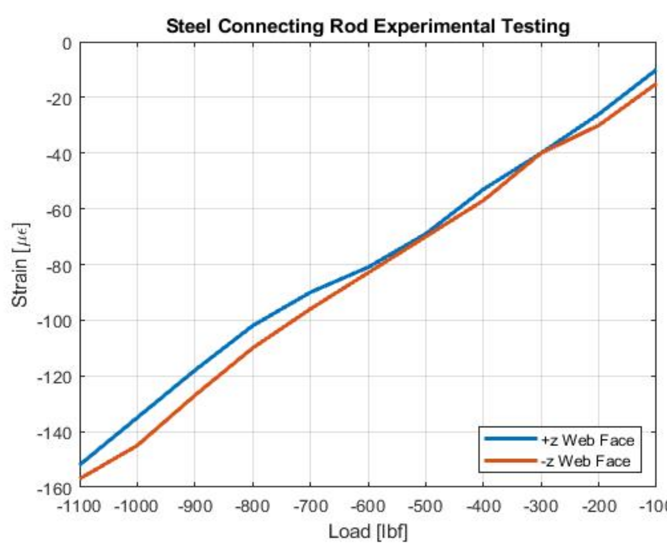

Figure 8 – Steel connecting rod compression data

2.2 FINITE ELEMENT METHOD

Finite element analysis was conducted using Abaqus CAE. The aforementioned CAD model was imported as a solid and meshed using C3D10 elements. Material properties applied to the geometry captured steel's elastic properties and are listed in Table 1. The primary region of interest is located within the web face of the I-beam section, 3" below the top of the piston end (smaller end) which corresponds to the same location of the strain gauges installed on the steel connecting rod. The results of the job and geometric naming convention are displayed in Figure 9 and the constraints, boundary conditions, and loading applied are as follows:

Table 1 – FEA material properties

Elastic Modulus	29 Msi
Poisson's Ratio	0.3

- Inner surface of piston end tied in all DOF to the center node of the diameter
- Inner surface of crank end tied in all DOF to the center node of the diameter
- Piston end center node zero displacement in X and Z and zero rotation about X and Y
- Crank end center node zero displacement in X, Y, and Z and zero rotation about X and Y
- -1000 lbf concentrated load applied at piston end center node in Y direction

When FEA strain results in the axial direction are compared with the data recorded from experimental testing a total error of 8% is produced. This shows that the modeled geometry is accurate to an acceptable level and will produce a machined component. Many sources of accumulated error could have attributed to this deviation such as slight geometric modeling differences, strain gauge location, and strain gauge alignment.

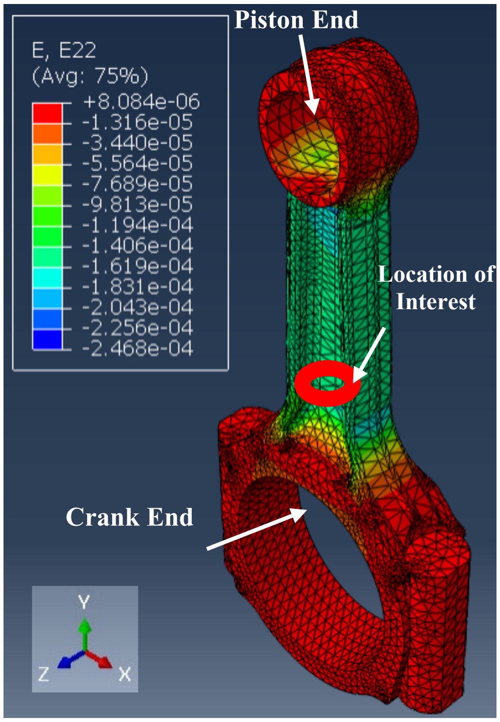

Figure 9 – Abaqus results

3. MOLD AND CURE PROCESS DEVELOPMENT

Compression molding was pursued based on heritage in high performance, high strength manufactured components. The compression molding process ensures a maximization of material volume and limiting of void content when executed properly. In order to maintain maximizing the amount of material composing the final machined component a brick compression mold was elected for a path forward. This would allow for minimal void content, cured shape control, and a consistent composite product which would be machined into the desired geometry.

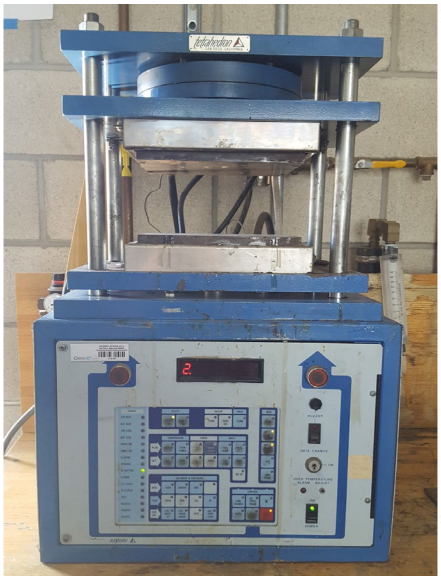

Figure 10 – Composite press

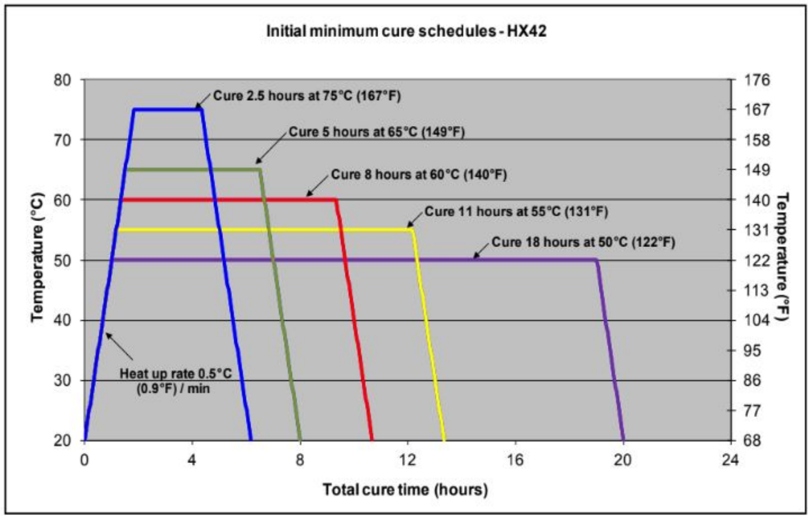

Figure 11 – Woven material cure profile [5]

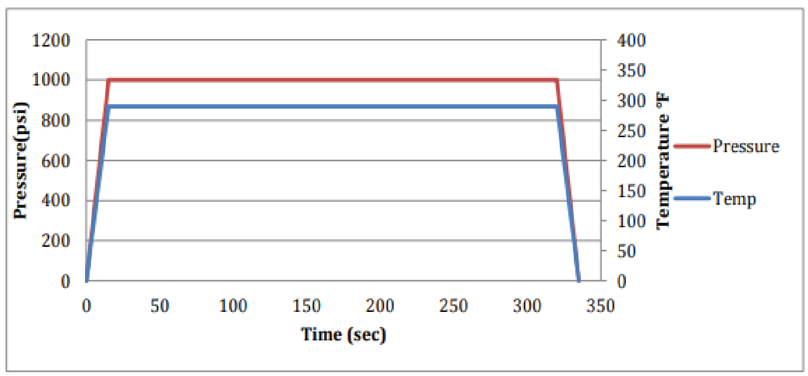

Figure 12 – Chopped fiber cure profile [6]

The composite materials utilized were cured using the Cal Poly Aerospace Engineering composite press (pictured in Figure 10). The cure cycle for the triaxially woven material can be seen in Figure 11 while the chopped fiber material's is pictured in Figure 12. The shortest cure cycle for the HX42 (Figure 11) was elected to allow for rapid iterating and production.

3.1 High Density Foam

Initial block cure tests conducted utilized high density foam (HDF) to create a constrained perimeter around material in an attempt to maintain post-cure shape. Temperature resistant vacuum bag tape was used to secure strips of foam to each other and an aluminum base plate. Each of the walls were sanded to within 0.05" of 0.86", which corresponds to the ultimate thickness of the brick necessary for the composite connecting rod geometry. The assembly along with the layup can be viewed in Figure 13. The composite was isolated from the upper and lower face aluminum plates using a non-porous teflon sheet.

Figure 13 – HDF mold attempt

The result of the cure cycle can be seen in Figure 14. This iteration revealed that the chopped material ran significantly due to discontinuous nature of the fibers. Additionally the pressure exerted on the heated vacuum tape and foam segments rotated the walls, thereby allowing the structure to be crushed edgewise and demolish the perpendicularity between the walls. Because of the issues of material containment and wall integrity a follow up iteration was conducted using medium density fiberboard (MDF).

3.2 Medium Density Fiberboard

As lateral constraints proved to be necessary to maintain perpendicularity between walls on the mold, MDF was elected for the next iteration. Segments were cut to the desired final brick height and screwed together after drilling pilot holes. Small cracks formed as a result of the screws being inserted, which propagated further after the cure as a result of the pressure applied from the composite press (visible in Figure 15). Although the mold stayed assembled, the cracks implied deformation in the thickness direction and caused concern about the repeatability of achieving the right thickness when curing machinable bricks. Because of the concern of consistency between cures, time was invested to machine a fully aluminum mold.

Figure 14 – HDF cure failure

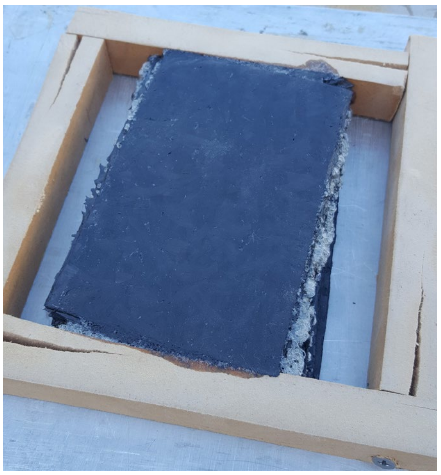

Figure 15 – MDF mold attempt

3.3 Aluminum Mold

The final mold design was a fully aluminum mold constrained in all directions. This was accomplished using ¼”-20 bolts which constrained the walls to each other, as well as through the thickness of the face plates and walls. This allowed for the max compression of material into the mold volume and voided the need to use the composite press, allowing for oven cures which provide a more consistent distribution of heating. The walls of the mold measured a height of 1”, so to ensure the target thickness of cured bricks a plate with an area of the inside walls of the mold was bolted to the underside of the top plate to ensure the proper thickness offset. The assembly after preparation for a brick cure is shown in Figure 16. The faces exposed to contact with the composite being cured were polished up to 800 grit to ensure a good material finish and ease of freeing the cured part. Mold release wax was applied to similarly facilitate easy part removal. The aluminum segments were soaked in paint stripper after cures to allow for the surfaces to be fully cleaned and any cured resin bleed into threading to be removed.

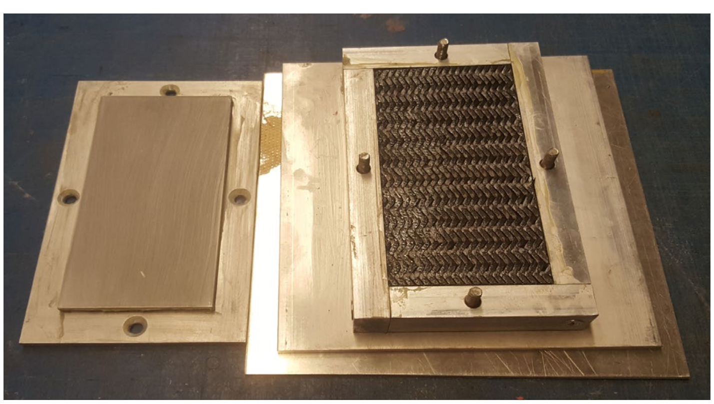

Figure 16 – Aluminum mold prepped for cure

4. MATERIAL MACHINABILITY AND TESTING

Multiple composite options were examined with consideration to their quality after curing, bleed-out of resin, and machinability. The two primary candidates examined were a pre-impregnated chopped carbon fiber with vinyl-ester matrix (Quantum AMC 8593 [6]) and a carbon fiber triaxial weave with epoxy matrix (Tencate AmberTool HX42 [5]). Each material's quality was inspected visually after curing for attributes which would benefit a compression molding process, and tested using ASTM D3039 [7] and D3410 [8] standards to characterize mechanical material properties. Compression mold repeatability was explored and used to assert a process for consistent brick molding.

4.1 Machinability

Machining the two composites was executed using carbide steel tools selected based on the necessary minimum dimensions necessary in the connecting rod geometry. The compression spiral tool was elected to have a diameter of 0.31” to maximize the removal of material from large areas of the brick where volume was not critical to part geometry, but still allow for the tool to be used in I-beam channels and end bores. A compression spiral tool was selected based on its ability to prevent delamination between composite plies. A 0.118” ball end tool was selected based on the radius of fillets in part geometry. The two tools are pictured in Figure 17.

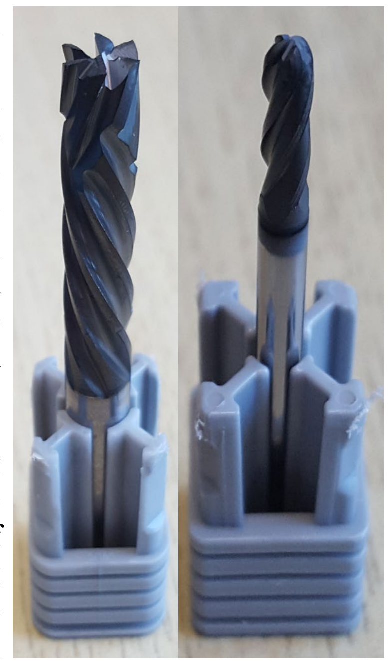

Figure 17 – Compression spiral (left) and ball end mill (right) cutters

To gauge the quality of machining on the two materials being explored an arbitrary geometry capturing similar cuts to the connecting rod was generated in MasterCAM. Two samples of 2”x2” were cut from bricks cured during the iterative molding process. Cutter speed was set to maximum (4000 RPM) as the Haas Mini-Mill being used could not achieve the material manufacturer recommended machine settings.

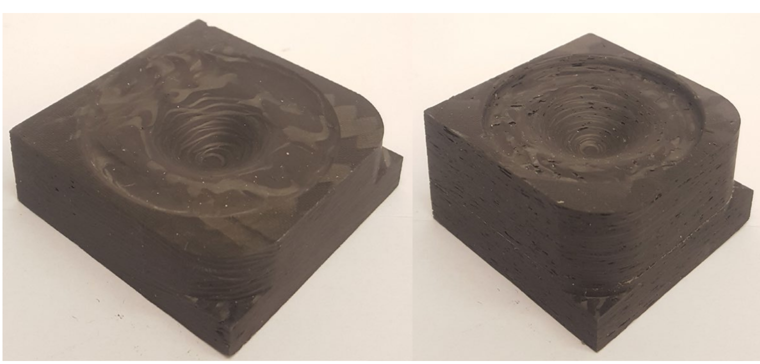

Figure 18 – Woven (left) and chopped fiber (right) machined samples

The two samples machined are exhibited in Figure 18. The chopped fiber sample produced visible defects in the form of chips. These were sections of the discontinuous fibers which were separated from the matrix and formed unpredictable divots of all sizes and depths. In contrast, the woven material maintained an excellent finish with no blemishes and a smooth surface.

4.2 Mechanical Property Testing

Materials were tested in both tension and compression using ASTM standards. 26 samples of the woven material and 5 of the chopped fiber were made from flat plates cured in the composite press and instrumented with strain gauges. Testing was conducted to failure for each specimen to characterize the expected elastic modulus and ultimate strength of each material. The results of each group of test specimen were average to generate a generalized value with acceptable standard deviation.

4.2.1 Coupon Preparation, Instrumentation, and Testing Procedure

Tensile coupons for both materials were manufactured according to the ASTM recommendations of a 1” by 0.1” cross section, and cut to a length of 10.5” based on the area constraints of the hot press used. Compression coupons were sized to the same cross sectional area and cut to a total length of 5”. Glass-epoxy tabs were cured to the ends of samples using a structural film adhesive to ensure a gripping surface for the hydraulic grips on the Instron testing machine. After tab attachment strain gauges were installed on each specimen using the procedure and materials provided in the M-Bond 200 adhesive kit [9]. The woven coupons instrumented with gauges are depicted in Figure 19. These coupons are a second set of test specimen created after a calibration issue was discovered, which will be discussed shortly.

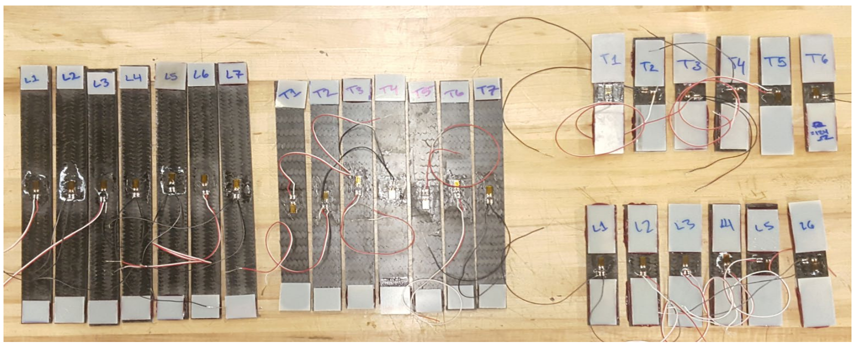

Figure 19 – Woven composite test coupons

4.2.2 Chopped Fiber Results

A total of 5 chopped fiber samples were tested: 2 tensile coupons and 3 compressive coupons. Limited number of samples available stemmed from the inability to control cure dimensions. Therefore the plates cured yielded only certain areas where the material stayed within tolerance in accordance with the ASTM recommended coupon dimensions. However, considering the preference of the woven material with respect to machining, the small sample size simply served as reinforcement to the expected failure characteristics. The data collected can be seen in Figures 20 and 21. Data collected for compression testing did not utilize strain gauges and instead calculated strain from the Instron crosshead position and sample gage length. However when compared to initial compression tests of a single woven compression coupon using a strain gauge the magnitude of the modulus appeared unrealistic. It was found that the machine was not calibrated and necessitated strain gauges on all samples for accurate data

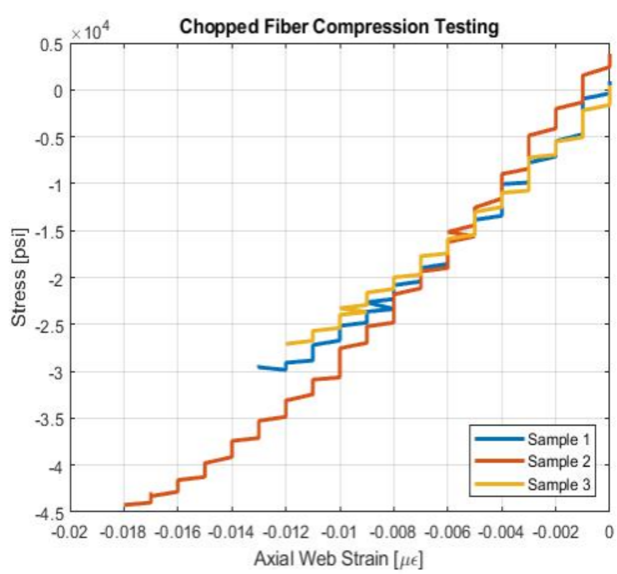

Figure 20 – Chopped fiber compression results

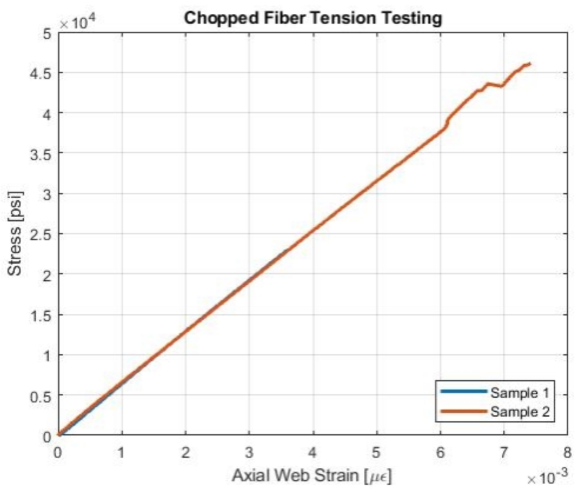

Figure 21 – Chopped fiber tension results

collection. Due to the difficulties experienced with producing consistent chopped fiber coupons the tests were not repeated.

4.2.3 Triaxial Weave Results

A total of 26 samples were manufactured for testing the woven material. 14 of these were split equally between the two orientations of interest with the 1 and 2 directions established in Figure 2 along the loading axis, while 12 (also split equally) were cut to size for compression testing. The results of these tests can be seen in Figures 22, 23, 24, and 25.

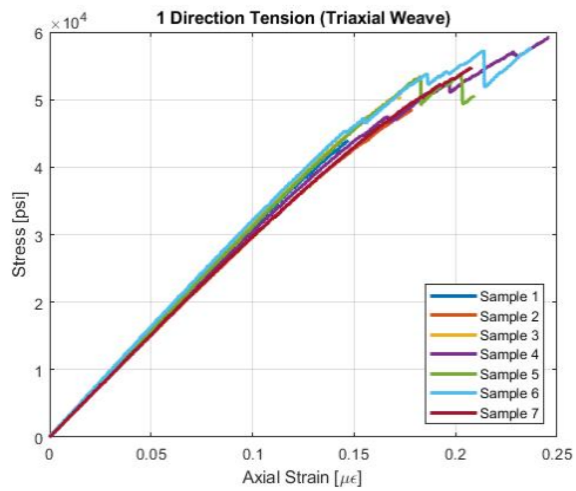

Figure 22 – Woven 1 direction tension results

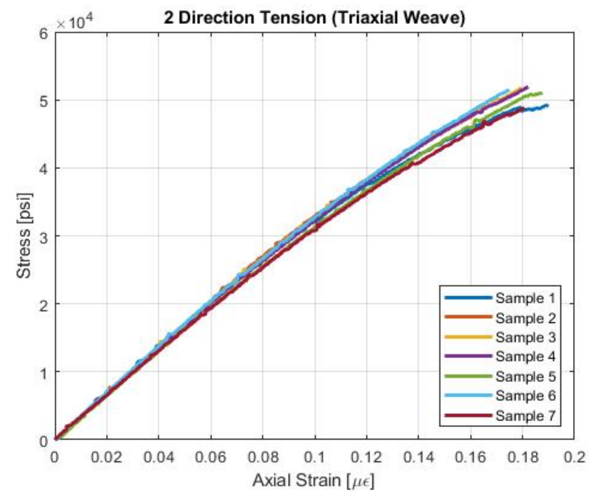

Figure 23 – Woven 2 direction tension results

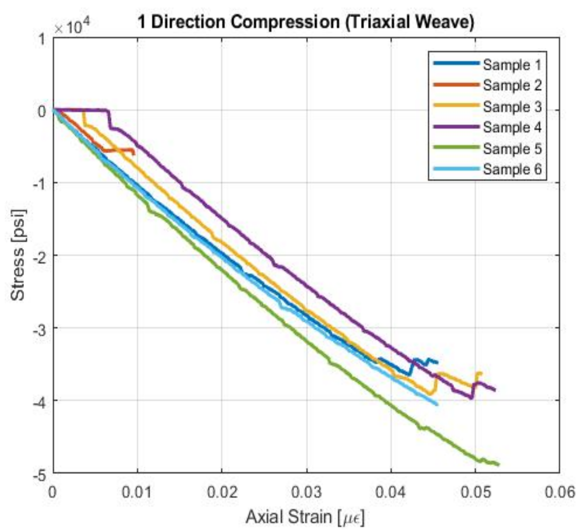

Figure 24 – Woven 1 direction compression results

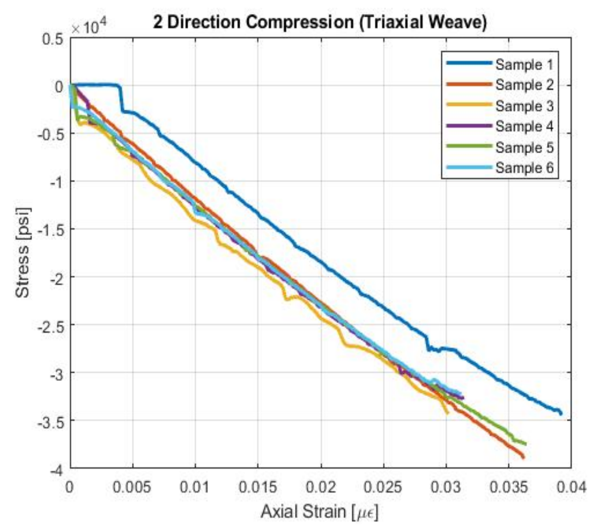

Figure 25 – Woven 2 direction compression results

The data collected showed a high level of correlation with exception to Sample 2 in the 1 direction compression tests. Therefore, this sample was removed for final averaging of ultimate strengths. The averaged results for all material tests are presented in Table 2 below.

Table 2 – Modulus and ultimate strength results

	Tension		Compression		Tension	Compression
	Woven 1 Direction	Woven 2 Direction	Woven 1 Direction	Woven 2 Direction	Chopped Fiber	
Average Young's Modulus [Msi]	0.27	0.29	0.84	1.02	6.37	2.58
Standard Deviation [Msi]	0.22	0.12	0.09	0.04	0.10	0.25
Average Ultimate Strength [ksi]	52.67	50.32	40.94	35.00	34.52	33.73
Standard Deviation [ksi]	5.36	1.64	4.72	2.69	16.33	9.21

As mentioned previously the data collected for the compression tests of the chopped fiber material were considered void. Although the results tabulated point to the material having superior performance in compression, these results cannot be trusted. Because of the aforementioned preference to the woven material in the context of machining and the difficulty to cure consistent chopped fiber test coupons material testing was halted for the material. Instead a single connecting rod would be machined from the material to allow for performance comparison against the woven material rods being focused upon.

5. COMPOSITE CONNECTING ROD MANUFACTURE AND TESTING

Based on the experimentation with respect to molding, machinability, and compressive elastic modulus it was asserted that the triaxially woven material would be ideal for composite connecting rod machining. Cures were conducted using the aluminum mold to produce 3 bricks of the woven material with the fibers oriented such that the 2 direction of the material was oriented with the axial loading direction of the component. A single chopped fiber block was cured such that a comparison in performance could still be made with the woven material.

5.1 Geometric Accommodations

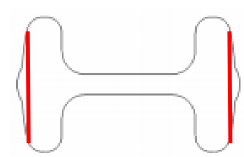

Figure 26 – I-beam cross section with modifications

To cut down machining time to the available access granted on a given day, and accommodate 3-axis milling constraints portions of the originally modeled geometry had to be adjusted. Figure 26 details how the I section of the body had to be adjusted. The red lines depicted show how the outer walls of the "I" were flattened as the originally curved geometry would have driven up the machine time significantly (beyond the hours available for machine access). In addition to the adjustment on the I-beam geometry an adjustment was required on the crank end. As exhibited in Figure 27 the original geometry at the bolt location

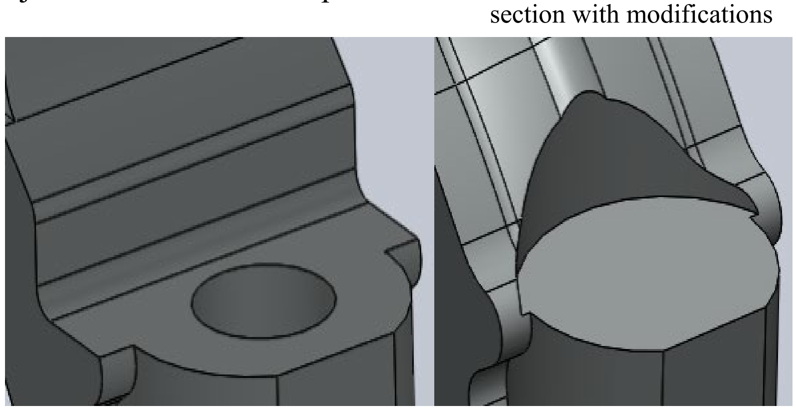

Figure 27 – Geometric accommodation (left) compared to original component geometry (right)

created negative drafts which were not physically possible to machine using the available equipment. Therefore the geometry was cleaned by squaring it and filleted to mitigate stress concentrations.

5.2 CNC Machining Process

CNC tool paths were generated and verified prior to machining using MasterCAM. Bricks were lightly sanded to clean edges and any extraneous material prior to being placed into the vice. The CNC process was split into two operations: OP1 containing the part roughing and finishing passes through half of the geometry in the part Z direction (pictured in Figure 28), and OP2 completing the geometry on the opposite half. The second operation therefore required an aluminum soft jaw matching OP1 geometry. Coolant was not used from the mill. Instead the cutter was intermittently sprayed with water to prevent overheating. To control carbon particulate a vacuum was kept pointed at the tool path which limited any airborne dust or contamination into the mill's moving parts.

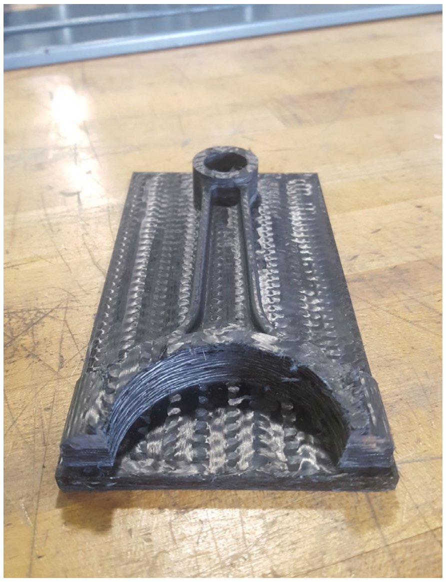

Figure 28 – Machined geometry after OP1

5.3 Post Processing and Test Preparation

After machining the geometry from carbon fiber it was necessary to clean frayed fibers using 250 grit sandpaper. The excess material was gently sanded to ensure that fibers from the main surfaces of the part were not delaminated. The crank end inner diameter was sanded more aggressively to remove the seam formed from the two operations of machining and ensure a smooth face for contact with the testing fixture. The piston end inner diameter similarly was sanded to remove any seam present and ensure easy insertion and removal of the pin for the testing fixture. Preparation for testing of the composite rod involved installation of a strain gauge to the inside surface of the web section at the same location as studied in the steel baseline case.

5.4 Compression Testing and Results

Testing of the composite connection rods consisted of three samples composed of the woven material in the previously defined orientation, and a single chopped fiber specimen for failure comparison. A woven rod with in its test configuration is visible in Figure 29. Prior to running destructive tests each specimen was run up to 800 lbf to compare trends and assert that strain gauge readings were not divergent. This data is displayed in Figure 30. It is observable that two of the woven rods exhibit nearly identical trends while the third has a slightly lower elastic modulus. In an attempt to troubleshoot this the strain gauge was reinstalled, however the results remained the same. It was assumed this discrepancy originated from either slight cross sectional area differences from machine tolerancing, quality control issues with the brick used for machining, or a combination of the two. Before running the failure tests the specimen were weighed to allow for a final strength to weight comparison. The weight of

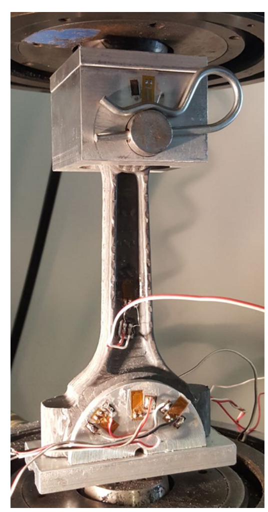

Figure 29 – Test configuration

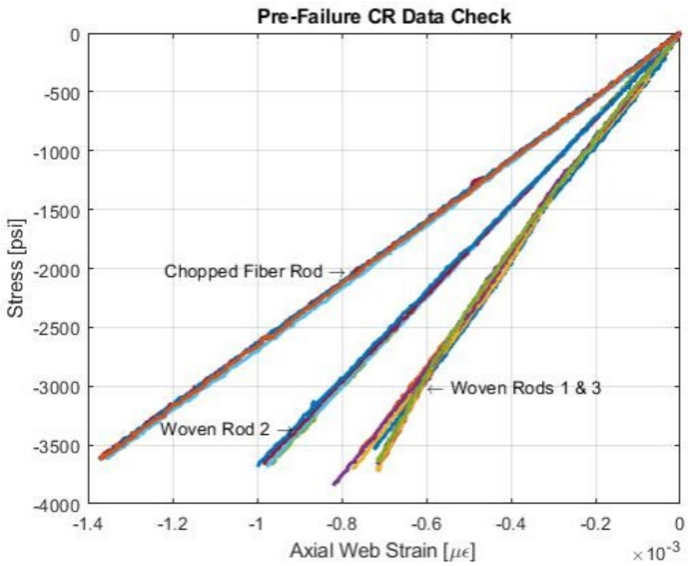

Figure 30 – Measurement verification

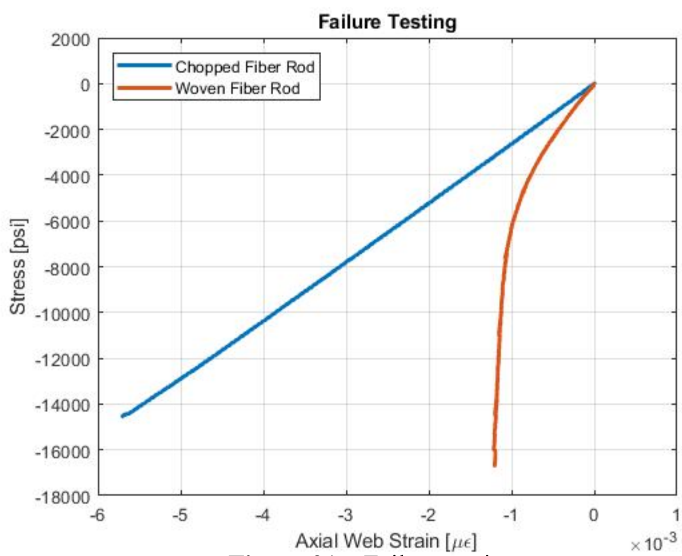

Figure 31 – Failure testing

Table 3 – Weight in lbs of connecting rods

Woven 1	Woven 2	Woven 3	Chopped Fiber	Steel
0.14375	0.1375	0.1375	0.11875	0.79375

the four rods tested and the steel baseline are tabulated in Table 3. The final destructive test data from a woven rod (Woven Rod 3) and the chopped fiber rod can be seen in Figure 31. Woven Rod 3 was selected based on its stiffness recorded during preliminary testing and its lower mass over Woven Rod 1 which exhibited the same stiffness. Note that the trend of the woven rod tested to failure is not linear. Although this is not ideal, loading and unloading the specimen several times could have impacted the failure strength and it was therefore elected to let the test run fully. The slope increases as the test gets into higher loading and could represent some level of material compaction or work hardening as the material enters the plastic region of deformation. The chopped fiber rod experienced a failure load of 3234 lbf while the woven rod experienced failure at 3720 lbf. These results are consistent with the trends ultimate strength differences found in material tests conducted previously.

The failure mode experienced by the chopped fiber rod is shown in Figure 32. This can be compared with the failure mode of the woven rod portrayed in Figure 33.

Based on the ultimate load of the composite rods and their weight prior to

Figure 32 – Chopped rod failure

Figure 33 – Woven rod failure

failure a strength to weight metric was evaluated for each of the failed rods. This was then compared to the same metric for the steel component based on the upper limits for the yield strength of high strength steel [10]. The metric can be simplified to utilize the failure load by assuming the same cross sectional area of all the connecting rods through the I-beam. The results for experimental tests and the theoretical limit of the steel baseline are tabulated in Table 4 below.

Table 4 – Rod performance metric comparison

Woven Rod	Chopped Fiber Rod	Steel
27054.54545	27233.68421	17760

The mass of the composite rods shows great improvement over the original design with approximately 15% of the total steel component's weight. Impressively the composite alternatives show a strength to weight metric several times higher than that of the steel component, although the failure loads of the composite rods is still below the design load recommended for the steel component. This shows that the composite provides a feasible option which is worth further exploration.

6. CONCLUSIONS

Although testing proved the difficulties in quality control of composite cures and gathering accurate data in an experimental setting, a number of valuable conclusions can be drawn from the study conducted. The composite connecting rod alternatives performed exceptionally when compared to the original baseline steel component when comparing the strength to weight ratios achieved. The failure load of the rod may have been lower than that of the design criteria for the steel component, but the mass cost savings are so incredible that geometric improvements might be appropriate in the composite connecting rod with little impact to driving up the weight. This could help to eliminate the delamination which failed the specimen at high stress locations. Ultimately, there is much to explore especially with respect to other environment effects on the composite, but the savings shown in this study point towards an exciting alternative in component design.

7. REFERENCES

[1] "4 Reasons Why Composites Are Replacing Traditional Materials." Fortify, 24 Oct. 2018, 3dfortify.com/composites-replace-traditional-materials/.

[2] "VectorStock." VectorStock, www.vectorstock.com/royalty-free-vector/crankshaft-with-connecting-rod-piston-group-vector-3009853.

[3] "ACP Composites." ACP Composites, 2019, cdn.crockercommerce.com/0012-products/12183.jpg.

[4] "Wikipedia." Wikipedia, en.wikipedia.org/wiki/3D_composites#/media/File:Braids.png.

[5] "Tencate AmberTool HX42 Tooling Prepreg Data Sheet." Tencate Composites, www.tencatecomposites.com/media/12dfd8a6-93e0-4666-945c-72a8d7f18a25/ENNdXQ/TenCate%20Advanced%20Composites/Documents/Product%20datasheets/Composite%20tooling%20prepregs/Composite%20tooling%20prepregs/TenCate-AmberTool-HX42_PDS.pdf.

[6] Schulman, A. "Quantum AMC 8593." Bay City. *Print*.

[7] "ASTM D3039 / D3039M - 17." ASTM International - Standards Worldwide, ASTM International, www.astm.org/Standards/D3039. https://doi.org/10.1520/d3039_d3039m

[8] "ASTM D3410 / D3410M - 16." ASTM International - Standards Worldwide, ASTM International, www.astm.org/Standards/D3410.htm. https://doi.org/10.1520/d3410_d3410m-16

[9] "Strain Gage Installations with M-Bond 200 Adhesive." Vishay Precision Group, www.vishaypg.com/docs/11127/11127B127.pdf.

[10] "High Strength Steels." Automotive Worldwide, automotive.arcelormittal.com/repository2/Automotive_Product%20offer/HighStrengthSteels.pdf.